Article

TiO2 Nanoparticles Functionalized with Non-Innocent Ligands Allow Oxidative Photocyanation of Amines with Visible/Near-Infrared Photons

Alexander M. Nauth, Eugen Schechtel, Rene Dören, Wolfgang Tremel, and Till Opatz

J. Am. Chem. Soc., **Just Accepted Manuscript** • DOI: 10.1021/jacs.8b07539 • Publication Date (Web): 28 Sep 2018

TiO_2 Nanoparticles Functionalized with Non-Innocent Ligands Allow Oxidative Photocyanation of Amines with Visible/Near-Infrared Photons

Alexander M. Nauth,[a,†] Eugen Schechtel,[b,†] René Dören,[b] Wolfgang Tremel,*[,b] and Till Opatz*[,a]

[a] Institut für Organische Chemie, Johannes Gutenberg-Universität Mainz, Duesbergweg 10-14, D-55128 Mainz, Germany
[b] Institut für Anorganische Chemie und Analytische Chemie, Johannes Gutenberg-Universität Mainz, Duesbergweg 10-14, D-55128 Mainz, Germany

†These authors contributed equally to this work.

Abstract

Photosynthesis is an efficient mechanism for converting solar light energy into chemical energy. We report on a strategy for the aerobic photocyanation of tertiary amines with visible and near-infrared light. Panchromatic sensitization was achieved by functionalizing TiO_2 with a 2-methylisoquinolinium chromophore, which captures essential features of the extended π-system of 2,7-diazapyrenium (DAP^{2+}) dications or graphitic carbon nitride. Two phenolic hydroxy groups make this ligand highly redox-active and allow for efficient surface binding and enhanced electron transfer to the TiO_2 surface. Non-innocent ligands have energetically accessible levels that allow redox reactions to change their charge state. Thus, the conduction band is sufficiently high to allow photochemical reduction of molecular oxygen even with near IR light. The catalytic performance (up to 90% chemical yield for NIR excitation) of this panchromatic photocatalyst is superior to all photocatalysts known thus far, enabling oxidative cyanation reactions to the corresponding α-cyanated amines to proceed with high efficiency. The discovery that the surface-binding of redox active ligands exhibiting enhanced light harvesting in the red and near-IR region opens up the way to improve the overall yields in heterogeneous photocatalytic reactions. Thus, this class of functionalized semiconductors provides the basis for the design of new photocatalysts containing non-innocent donor ligands. This should increase the molar extinction coefficient, permitting a reduction of nanoparticle catalyst concentration and an increase of the chemical yields in photocatalytic reactions.

INTRODUCTION

Sunlight is an abundant source of energy which can drive chemical reactions in an eco-friendly fashion and is most likely to play a key role in the global energy supply of the future. Catalytic systems using visible (VIS) or infrared (IR) light are highly attractive because ultraviolet (UV) radiation accounts only for a small fraction of the sun's energy spectrum.[1–4] In fact, the maximum photon flux of the sun is centered around 880 nm, while its maximum power output is centered around 500 nm.[5] Most plants depend on sunlight and use the visible portion of the solar spectrum with the aid of photosynthetic pigments (e.g. tetrapyrroles and carotenoids).[6]

Chemists attempt to mimic the photosynthetic conversion of solar to chemical energy with photoredox systems and sensitizers. Irradiation leads to a photoexcited state that serves as a source of electrochemical potential.[4,7,8] The lifetime of the photoexcited state, the quantum efficiency of its formation, and the chemical stabilities of ground and excited state, have been exploited in the design of systems for solar energy conversion, either directly into electrical current, but also for electron-transfer reactions, where substrates can be oxidized or reduced, depending on the conditions. TiO_2 is a stable, non-toxic, low-cost material for photocatalysis,[9,10] whose photocatalytic efficiency is dictated by the charge separation efficiency, surface area, and exposed reactive facets.[11] Photoreduction with unmodified TiO_2 nanoparticles (NPs) requires UV light which reduces the efficiency of unmodified TiO_2 in solar applications.[12–14] Therefore, transition metal complexes,[15–17] organic dyes[18,19] or semiconductor nanoparticles[20] have been used as sensitizers in TiO_2-based solar cells. These surface-bound chromophores not only serve to shift the light absorption of unmodified TiO_2 particles from the ultraviolet to the visible region, but – in the case of "black dyes"[21–23] – achieve a panchromatic sensitization.[24] Among the concepts of TiO_2 sensitization *via* surface-bound chromophores, one particular approach has become popular in the last few years: Photosensitization through ligand-to-metal charge transfer (LMCT) on TiO_2 surfaces,[25] which has also been employed in dye-sensitized solar cells (DSSCs).[26,27]

In inorganic photocatalysis, the semiconductors ZnO,[28] ZnS,[29] CdQ (Q = S, Se, Te) quantum dots,[30,31] carbon nitride,[32] BiOBr,[33] or $PbAO_2X$ (A = Sb, Bi, X = Cl, Br[34]) with absorption in the visible range were used to maximize the efficiency of light utilization. Likewise, organic dyes[35,36] and inorganic pigments[21,37] were used to stretch to absorption into the visible range. Crucial for the TiO_2 catalyst performance are light-absorbing chromophores, which must be (I) thermo-, photo- and chemically stable. In addition, an efficient photocatalyst should (II) absorb strongly in the

ultraviolet–visible (UV–VIS) region to produce electrons and holes, (III) separate the electrons and holes in space to prevent their recombination, (IV) carry robust anchor groups for surface binding, (V) have a ground-state potential positive enough to facilitate hole transfer to the catalyst, and an excited-state potential more negative than the edge of the semiconductor conduction band to allow interfacial electron transfer.[32] It is difficult to fulfill all criteria (I)-(V) simultaneously.

TiO_2 nanoparticles sensitized with a variety of $Ru(bpy)_3^{2+}$ dyes are prototypical heterogeneous photocatalysts.[22–24,38] Although organic dyes find wide application as pigments, colorants, or photoreceptors, only a few have been utilized in photocatalysis, because they suffer from photodegradation on TiO_2 under visible-light irradiation.[39,40] Perylene bisimides[41] or metalated porphyrins[42] fulfill the stability requirements, optical and redox criteria,[38] when surface-bound *via* different anchor groups (e.g. carboxylic acids, phosphonic acids, hydroxamic acids, or silatranes).[43] However, these groups are typically redox-inert and do not allow efficient charge transfer. Polymeric carbon nitride (CN_x)-TiO_2 organic–inorganic heterojunction photocatalysts have shown promising photocatalytic activity for the degradation of organic dyes[44] or the photocatalytic generation of H_2.[45] However, their visible light harvesting capabilities are limited because they suffer from a weak interaction and poor electron transfer across the TiO_2 and the CN_x interface.

Here, we demonstrate that a novel redox-active chromophore bound to TiO_2 nanoparticles through strong electronic coupling fulfills all performance criteria and permits the panchromatic TiO_2 sensitization for efficient aerobic photocyanation of tertiary amines. To this end, we synthesized the 6,7-dihydroxy-2-methylisoquinolinium (DHMIQ) ligand containing the 2-methylisoquinolinium chromophore equipped with a redox-active catechol surface anchor group (Figure 1a). This new ligand combines the essential features of two known chromophores: (i) quinolinium cations (e.g. *N*-methyl-quinolinium (NMQ^+)) and (ii) 2,7-diazapyrenium dications (DAP^{2+}). NMQ^+ cations are powerful photocatalysts with strongly oxidizing and long-lived excited singlet states,[46,47] but their UV absorption range and their susceptibility to attack by nucleophiles in the 2- and 4-position render them unsuitable for photocyanation. 2,7-Diazapyrenium dications (DAP^{2+})[13,48] with an extended isoquinolinium-type π-system absorb in the visible range and do not suffer from nucleophilic attack on the chromophore. The catechol surface anchor makes the ligand highly redox-active ("non-innocent"[49–51]) by facilitating efficient electron transfer to/from the metal oxide surface.[52,53]

Nature employs non-innocent ligands in various metalloenzymes where the active site contains a redox-active ligand that works in synergy with a metal center.[54,55] These ligands have more

energetically accessible levels that allow redox reactions to change their charge state. The functionalized TiO_2 nanoparticles exhibit a substantially improved vis-NIR spectral light harvesting performance compared to pure CN_x[44] or unfunctionalized naked TiO_2 nanoparticles. Neither unfunctionalized particles nor the sensitizer itself show any appreciable light absorption in the visible spectral range. The surface-functionalized particles, however, allow direct photocatalysis down to the near-infrared region.[56,57]

The catechol-bound isoquinolinium chromophore is particularly suited because (i) amines and cyanides do not absorb visible light and therefore cannot be excited directly, (ii) direct oxidation of organic substrates with molecular oxygen is kinetically unfavored.[58] (iii) The redox potentials of functionalized TiO_2 particles are comparable or even higher than those of typical photoredox catalysts like $Ru(bpy)_3^{2+}$.[59] This enables the use of oxygen as terminal oxidant and circumvents the use of stronger or kinetically faster oxidants like ClO_2, H_2O_2, *t*-BuOOH, or carbenium ions. (iv) The redox potential of the TiO_2-DHMIQ system is utilized for single-electron oxidations[60] of the amines and the subsequent addition of cyanide to the iminium ion resulting from hydrogen abstraction.

We have applied these new photocatalysts for the synthesis of α-aminonitriles by oxidative cyanation. α-Aminonitriles are an important class of compounds for the synthesis of nitrogen-containing bioactive compounds like α-amino acids and alkaloids or heterocycles.[61–63] Their various modes of reactivity make them versatile and widely applicable intermediates in organic chemistry[64] since the nitrile function can either be transformed to carboxy, amide, or aminomethyl function or be completely replaced by alkyl or aryl groups in single operation.[65] This also makes α-aminonitriles ideal intermediates in the postfunctionalization of amines. In this paper, we demonstrate oxidative cyanation of tertiary amines catalyzed by TiO_2 particles functionalized with the novel redox-active chromophore, the scope of the reaction and the basic reaction mechanism.

RESULTS AND DISCUSSION

First, the 6,7-dihydroxy-2-methylisoquinolinium chloride surface ligand (Figure 1a) was synthesized from homoveratrylamine (**1**), which was converted with formaldehyde in a combined Pictet-Spengler/Eschweiler-Clarke reaction to 6,7-dimethoxy-2-methyl-1,2,3,4-tetrahydroiso-quinoline (**2**) (Figure 1b).[66] After oxidation with 2,3-dichloro-5,6-dicyanobenzoquinone (DDQ) to 6,7-dimethoxy-2-methylisoquinolinium chloride (**3**), DHMIQ was obtained by acidic cleavage of the

methyl ethers. In the second step, TiO_2 nanoparticles were prepared hydrothermally from titanium(IV) butoxide with oleic acid and oleylamine in ethanol,[67] yielding nanoparticles of spherical to elongated shape and a typical size on the order of 10 nm (Figure S1). Powder X-ray diffraction confirmed that the particle cores consist of the anatase phase of TiO_2 (Figure S2). The as-synthesized TiO_2 particles carry oleate capping ligands (TiO_2-OA) and are perfectly soluble in apolar solvents like $CHCl_3$, *n*-hexane or tetrahydrofuran (THF). The outstanding solubility allows for nuclear magnetic resonance (NMR) investigation of the nanoparticle's ligand sphere. Thus, the ^1H NMR spectrum of as-synthesized TiO_2-OA NPs (Figure S3) confirms the presence of oleic acid as surface ligand. The surface-bound ligands give rise to signal broadening.[68] Re-functionalization of TiO_2-OA with the positively charged DHMIQ ligand rendered the nanoparticles water-soluble, inducing a polarity umpolung of the nanoparticle's ligand sphere (Figure 1c). The DHMIQ-functionalized TiO_2 nanoparticles were purified by repeated cycles of dissolution, precipitation and drying to remove displaced OA and excess DHMIQ molecules. No significant change in size, shape, or phase of the particles was observed after the ligand exchange (Figures S1 and S2). ^1H NMR investigation of surface-modified TiO_2-DHMIQ NPs in D_2O (Figure S4) revealed a virtually complete displacement of native OA ligands, indicated by the loss of the aliphatic signal in the high-field regime of the spectrum. The spectrum is dominated by two intense and rather broad signals, which can be assigned to the partially coalesced signals of DHMIQ. The NMR data reveal that the ligand spheres of the particles consist predominantly of single molecule species before and after surface modification. Therefore, it is possible to estimate the surface coverage of the ligands simply by quantifying the organic fraction of the nanoparticles *via* thermogravimetric analysis (TGA, Figure S5). By combining the TGA data with the particle dimensions (Figure S1), ligand densities of 2.4 ± 1.0 nm^{-2} for TiO_2-OA and 2.0 ± 0.9 nm^{-2} for TiO_2-DHMIQ NPs were obtained (Table S1). The surface density of the OA ligand is lower than for other oleate-stabilized NPs due to the purification (removel of unbound ligand) of the as-synthesized TiO_2 NPs.[69] The same applies for the DHMIQ-modified NPs since most ligand exchange studies with catechol derivatives have yields usually twice as high.[70]

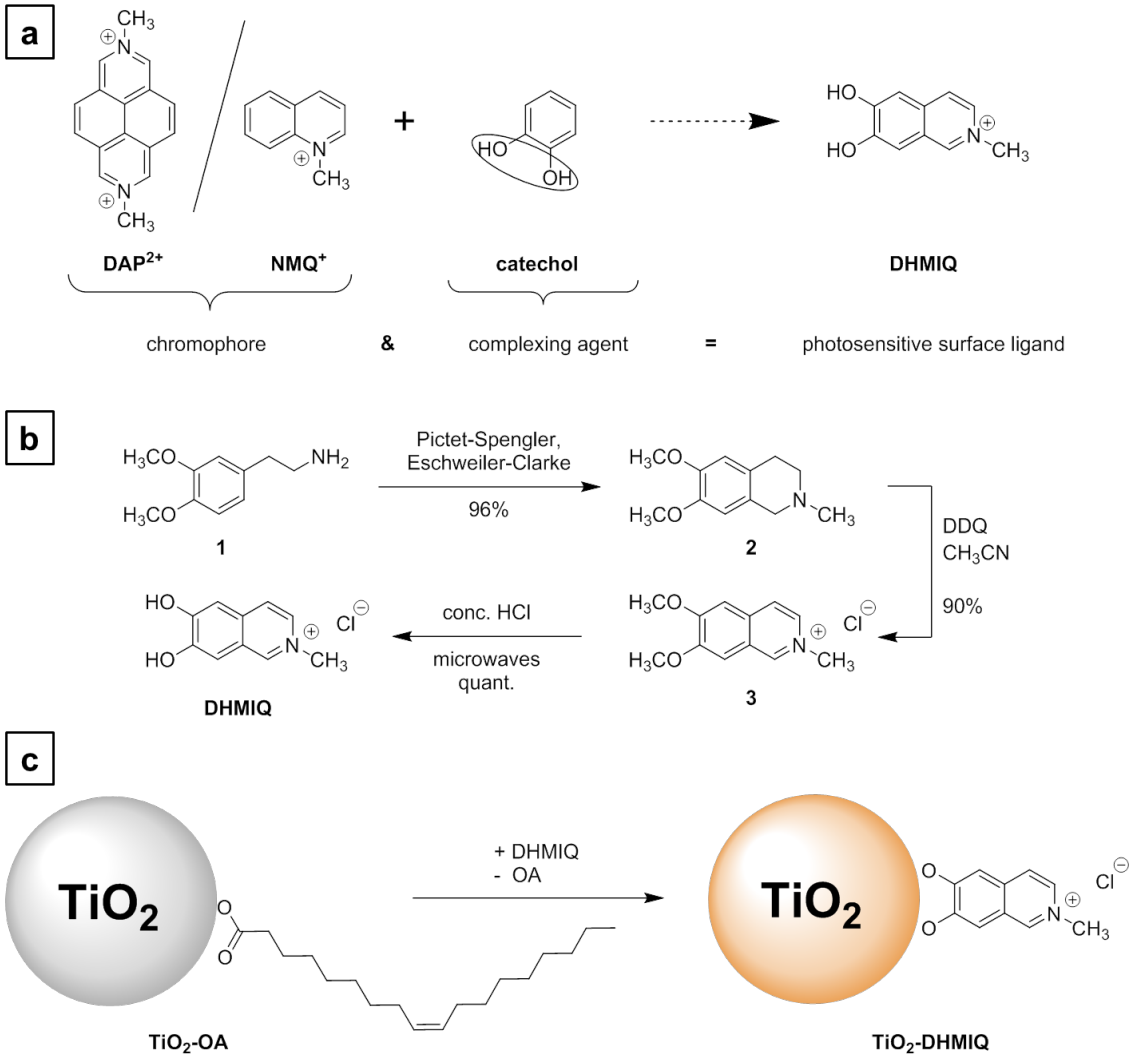

Figure 1. Design and synthesis of DHMIQ-sensitized TiO_2 nanoparticles. (a) Combination of the organic photocatalyst (*N*,*N*'-dimethyl-2,7-diazapyrenium (DAP^{2+}) or *N*-methyl-quinolinium (NMQ^+)) and the complexing agent catechol to yield the photosensitive surface ligand DHMIQ. (b) Synthetic route for the preparation of DHMIQ from homoveratrylamine (**1**). (c) Sensitization of TiO_2 NPs *via* postsynthetic ligand exchange of oleic acid (OA) with DHMIQ.

The large specific surface area (~150 m^2g^{-1}, Table S1) of the anatase nanoparticles aids in the formation of a photocurrent, similar as in DSSCs that operate based on similar principles.[38,39] The functionalized TiO_2 nanoparticles show a substantially enhanced solar light harvesting performance compared to "naked" TiO_2 nanoparticles. Band gap excitation of TiO_2 efficiently utilizes the optical spectrum (band gap of 3.2 eV for anatase TiO_2 with the conduction band starting close to the redox potential of the normal hydrogen electrode).[71] A significant portion of the visible and even the NIR spectrum (Figure 2a) is utilized with the TiO_2 surface-bound isoquinolinium ligand.

Upon photo-excitation of the ligand, electron transfer occurs from the ligand LUMO to the TiO_2 conduction band (Figure 2b).

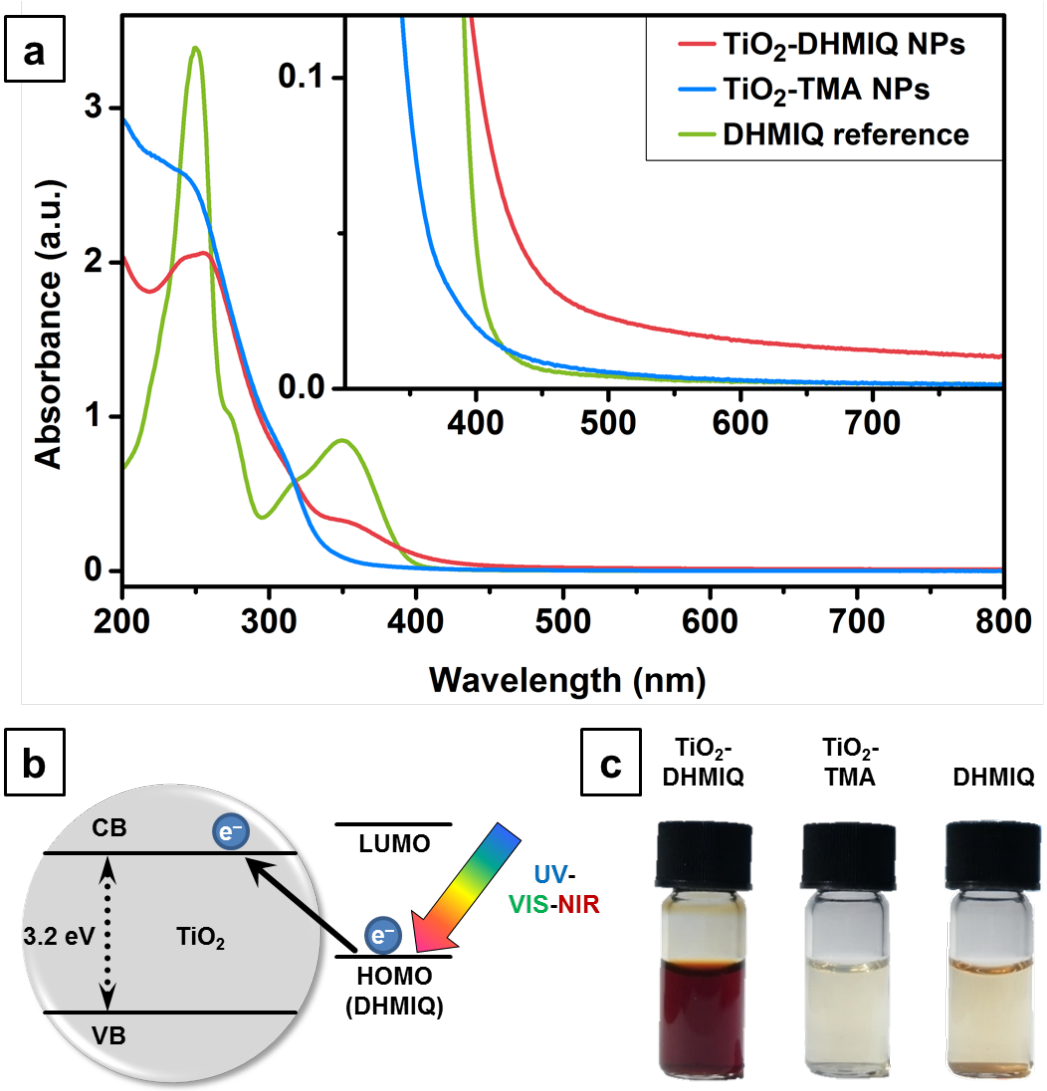

Figure 2. Light-absorbing properties of DHMIQ-sensitized TiO_2 nanoparticles. (a) UV/Vis absorbance spectrum of TiO_2-DHMIQ NPs (red line) in comparison with ligand-stripped TiO_2 NPs (with tetramethylammonium (TMA) counterions, blue line) and a pure DHMIQ reference (green line). The inset shows the enlarged Vis-NIR absorption range where the charge transfer in TiO_2-DHMIQ NP takes place. (b) Proposed excitation scheme for DHMIQ-sensitized TiO_2 nanoparticles (CB: conduction band, VB: valence band, LUMO: lowest unoccupied molecular orbital, HOMO: highest occupied molecular orbital). (c) Visual appearance of DHMIQ-sensitized TiO_2 NPs (left), ligand-stripped TiO_2 NPs (middle), and DHMIQ reference (right) in aqueous solutions. Nanoparticle concentrations of TiO_2-DHMIQ and TiO_2-TMA: 100 mg/mL, DHMIQ reference concentration: 12 mg/mL.

In order to demonstrate that the wide-ranging absorption of TiO_2-DHMIQ nanoparticles arises specifically from the surface complexation, a reference batch of ligand-stripped, water-soluble TiO_2 NPs was prepared by reacting TiO_2-OA NPs with tetramethylammonium hydroxide (TMAH).[72,73] As can be seen by NMR spectroscopy (Figure S6), the hydroxide treatment displaced the native

oleate ligand quantitatively, leaving a negatively charged TiO_2 nanoparticle surface, stabilized electrostatically by the counterion tetramethylammonium (TMA). Due to the non-coordinating nature of the TMA cation, TiO_2-TMA (Figure 2a) exhibits no charge-transfer band at ~360 nm, and strong absorption only occurs below 350 nm for TiO_2-TMA, which is a typical feature of non-sensitized TiO_2 nanoparticles.[74] The unbound DHMIQ ligand has two absorption bands centered at 251 and 351 nm. The DHMIQ-functionalized TiO_2 particles show absorption throughout the visible range and tailing into the near-infrared (Figure 2c), while non-sensitized TiO_2 particles or the unbound ligand show no significant absorption in the visible range (inset in Figure 2a). The catechol group of the DHMIQ ligand acts as the docking site for binding to the TiO_2 surface because the absorption spectrum is red-shifted after the binding of DHMIQ, which indicates the electronic interaction of the chromophore with the TiO_2 NPs. The broad absorption of the TiO_2-DHMIQ NPs is attributed to diverse interactions across the ligand-NP interface: (i) The non-innocent, redox-active nature of DHMIQ allows for a multitude of electronic and associated redox states with diverse electronic transitions. (ii) Multiple facets of the nanocrystals and a non-negligible density of intrinsic surface defects in hydrothermally synthesized TiO_2 NPs[75] lead to a multitude of complexation geometries with different excitation energies.

The energy conferred by infrared light excitation is limited by the energy of the absorbed photons. The energy of near-infrared photons (800 nm) of 1.6 eV (149 kJ/mol) is the maximum theoretical energy threshold between the photocatalyst and the acceptor. Since a part of this energy is lost due to intersystem crossing or reorganization of the excited states of the photocatalyst by non-radiative pathways, the maximum available energy of TiO_2-DHMIQ is in the order of 100 kJ/mol and still sufficient for oxidizing tertiary amines. The α-cyanation of tertiary amines reported here is one of the few[36,76] catalytic applications based on photoinduced interfacial electron transfer between a non-innocent ligand covalently bound to a TiO_2 NP surface.

The catalytic activity for the oxidative cyanation of different amines in the presence of trimethylsilyl cyanide (TMSCN) was examined. In a typical reaction, an aliquot of the aqueous catalyst solution was transferred into a reaction vial and freeze dried. The dried catalyst was suspended in acetonitrile, the amine substrate was added, and the solution was saturated with oxygen. After adding TMSCN as a cyanide source, the solution was irradiated (Figure S7). The crude cyanation product was isolated by extraction and purified by column chromatography. The minimum amount of catalyst required for nearly quantitative yield was determined by successively increasing the catalyst loading in a series of otherwise identical reactions (Figure S8). A catalyst loading of 2.5 mg TiO_2-

DHMIQ NPs, corresponding to 0.6 mol% of the catalytically active LMCT complex with respect to the standard amount (0.24 mmol) of substrate, was found to be sufficient. Trace amounts of water in the reaction mixture caused considerable losses in yield. A systematic study revealed that increasing amounts of water caused an exponential decay in reaction yield, levelling out at 20% (Figure S9). The most plausible explanation for this behavior is the formation of a hydration shell around the polar nanoparticles in the otherwise aprotic environment of acetonitrile which passivates the surface and leads to an energy barrier for the surface reactions.[77] Since the hydration shell has a finite maximum thickness, the conversion is not completely suppressed for higher amounts of water (see Section 5.2 in SI for a more thorough discussion).

Table 1. Yields of the photocatalytic oxidative cyanation of tributylamine, using as-synthesized TiO_2-A NPs, ligand-stripped TiO_2-TMA NPs, DHMIQ-sensitized TiO_2 NPs and unbound DHMIQ as photocatalysts for different excitation wavelengths (LED source) and excitation powers.

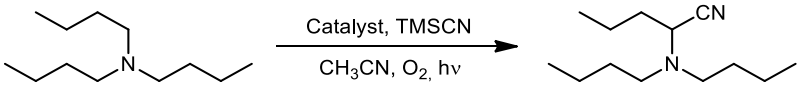

4 5

Light source	LED blue 462 nm, 100 W	LED green 520 nm, 100 W	LED yellow 592 nm, 52 W	LED red 635 nm, 67 W	LED IR 1 730 nm, 51 W	LED IR 2 850 nm, 3.7 W
TiO_2-OA	43%[a]	13%[a]	<1%[a]	×	×	n.t.
TiO_2-TMA	4%[a]	2%[a]	×	×	×	n.t.
TiO_2-DHMIQ	$96\%_{isolated}$	93%[a]	56%[a]	43%[a]	19%[a]/61%[a, b]/90%[d]	2%[a]/12%[a, c]
DHMIQ	84%[a]	22%[a]	2%[a]	<1%[a]	×	×
Background	15%[a]	3%[a]	×	×	×	×

Conditions: Bu_3N (0.239 mmol, 1.0 eq.) and TiO_2-DHMIQ NPs (2.5 mg) were dissolved in CH_3CN (4.0 mL) the solution was saturated with O_2 and TMSCN (3.0 eq.) was added. Unless stated otherwise, irradiation time was 3 h. Yield was determined by ^1H NMR using 1,4-bis(trimethylsilyl)benzene as an internal standard. [a]Incomplete conversion. [b]14 h reaction time. [c]16 h reaction time. [d]62 h reaction time.

Different excitation wavelengths were tested to excite the TiO_2-DHMIQ photocatalyst. Nearly quantitative yields were achieved after 3 h reaction upon irradiation with blue and green light (96% and 93%, see Table 1). The conversion decreased for excitation with yellow, red and NIR (730 nm) light. However, this could be compensated by using longer irradiation times (90% yield after 62 h irradiation for NIR). It is unusual and quite extraordinary that even IR radiation at 850 nm from a relatively weak 3.7 W LED module resulted in a conversion of 12% after a 16 h reaction period. This is consistent with the very broad absorption spectrum of the TiO_2-DHMIQ photocatalyst. Controls with free DHMIQ gave much lower yields under identical conditions and for ligand-stripped TiO_2-TMA NPs, the yields were almost zero. This demonstrates that covalently functionalized

TiO_2 nanoparticles are essential for the oxidative cyanation reaction under visible and NIR light. Finally, recyclability studies revealed that the heterogeneous photocatalyst could be recovered and reused several times, with the yield decreasing only moderately from 95% to 82% after four cycles of photocatalysis (Figure S10).

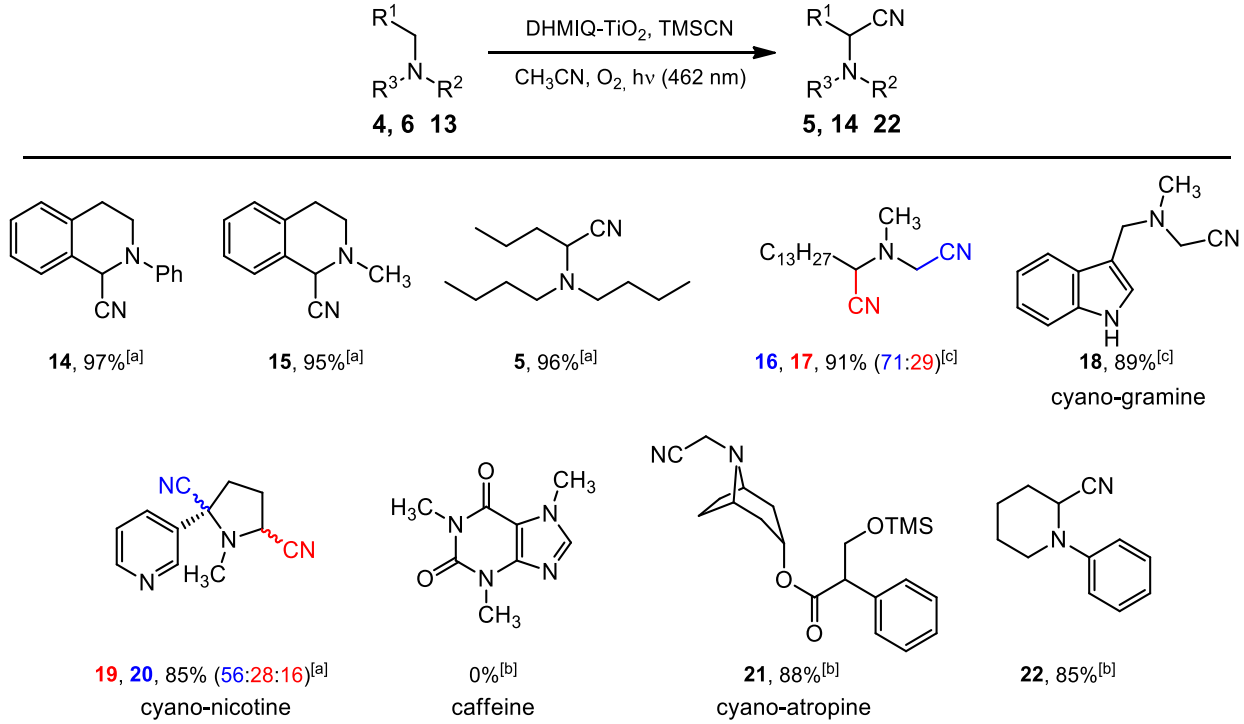

Figure 3. Visible-light/NIR induced oxidative cyanation of amines into α-aminonitriles with O_2 on DHMIQ-sensitized TiO_2 NPs. Yields were isolated. Reaction conditions: [a]3 h. [b]16 h. [c]24 h. Structures verified by ^1H and ^{13}C NMR (Figures S11-S43).

To demonstrate the substrate scope of TiO_2-DHMIQ, the catalyst was applied to a variety of different tertiary amines (Figure 3). Besides simple aliphatic amines like tributylamine, complex natural products like nicotine and atropine were also converted into their corresponding α-aminonitriles and isolated in remarkable yields. The hydroxyl group of atropine was TMS-protected due to the effect of TMSCN as a silylating agent. Reactions with the TiO_2-DHMIQ catalyst led to different cyanation products compared to those using the organic dye rose bengal as photocatalyst. For nicotine, cyanation occurred in the benzylic position with TiO_2-DHMIQ while rose bengal favors a reaction at the methyl group.[19] For *N*,*N*-dimethyltetradecylamine, the unexpected formation of 2-(dimethlyamino)pentadecannitrile was observed with TiO_2-DHMIQ, and the yield of the cyanation of the *N*-methyl groups of gramine was approx. 4.5 times higher than that with rose bengal (89% vs. 20%).[19] This differential selectivity could prove useful in further synthetic endeavors. In

addition, reactions with the TiO_2-DHMIQ catalyst appeared to be milder than those with rose bengal, as the isolated crude products were of superior purity.

With the catalytic activities, the results of the control experiments and the structure and properties of molecular Ti(IV) complexes[78] and TiO_2 particles functionalized with catechol ligands[79] a tentative mechanism of visible-NIR light photoredox catalysis with DHMIQ-sensitized TiO_2 nanoparticles is proposed in Figure 4. The DHMIQ chromophore is anchored on the TiO_2 particle surface with a catechol group to form a stable LMCT complex. Upon irradiation, DHMIQ is excited and a charge transfer occurs to the TiO_2 nanoparticle, which is associated with an injection of an electron into the TiO_2 conduction band. In the next step, the electron reacts with O_2 at the TiO_2 surface to form a hyperoxide radical anion $O_2^{\bullet-}$.[10] The $O_2^{\bullet-}$ radical anion displaces CN^- from TMSCN to form a TMS-peroxo species which then abstracts a H-atom from the amine radical cation to generate an iminium ion.[80,81] To elucidate the fate of the TMS-peroxo species, a reaction mixture was investigated by ^{29}Si NMR spectroscopy after irradiation. The ^{29}Si NMR spectrum (Figure S44) revealed the presence of four major Si-containing products, all of them different from TMSCN (Table S6). The two most prominent signals can be safely assigned to trimethylsilanol TMSOH and its condensation product hexamethyldisiloxane $(TMS)_2O$. The other two species are most probably bis(trimethylsilyl) peroxide $(TMSO)_2$ and trimethylmethoxysilane (Table S6). As a mechanistic alternative for iminium formation, α-amino radical intermediates are often discussed in the literature.[82] These might be formed by α-deprotonation of the amine radical cations[83,84] or through H-atom transfer[85] from the parent amine. Since neither the addition of diethylsilane (whose Si–H bonds are slightly weaker than the C_α–H bonds of trialkylamines) nor the addition of ethyl acrylate as a known trap for α-amino radicals[86–88] interferes with the clean photocyanation of tributylamine (see the SI for details), both alternatives appear unlikely. Increasing the size of the silyl group from TMS to *tert*-butyldimethylsilyl (TBDMS) slows down the photocyanation, but only leads to minor changes in the regioselectivity (**16**/**17** and **19**/**20**, see Section 7.2 in the SI for details). Further experimental and theoretical work is needed to obtain a deeper mechanistic insight.

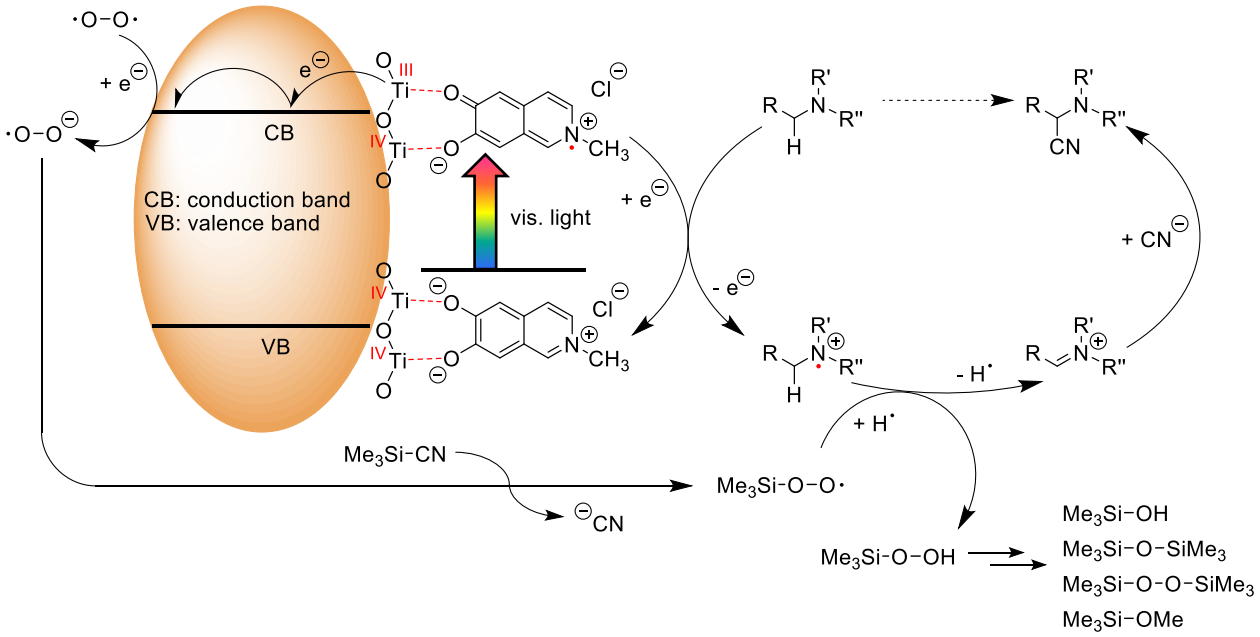

Figure 4. Proposed mechanism for the visible-light-induced oxidative cyanation of tertiary amines with O_2, catalyzed by DHMIQ-sensitized TiO_2 nanoparticles.

From a mechanistic point of view, the TiO_2-DHMIQ system is not only responsible for visible light harvesting, but is also the driving force for the oxidative transformation. Compared to similar aerobic oxidation reactions, this double functionality obviates the need for an additional redox mediator such as (2,2,6,6-tetramethylpiperidin-1-yl)oxyl (TEMPO)[36,76,89] or a radical initiator such as azobisisobutyronitrile (AIBN).[63] Furthermore, the heterogeneous nature of the catalyst enables an easy recovery, which makes the TiO_2-DHMIQ system a superior photocatalyst for oxidative cyanation and a promising candidate for other oxidative transformations.

CONCLUSION

A redox-active DHMIQ ligand was prepared for surface sensitization of TiO_2 nanoparticles. It allows panchromatic sensitization for photocatalytic oxidative cyanation reactions using molecular oxygen as oxidant. This photo-active DHMIQ ligand was adsorbed onto TiO_2 nanoparticles *via* postsynthetic quantitative ligand exchange of oleic acid, yielding a DHMIQ ligand density of 2.0 ± 0.9 nm^{-2}. The ligand, when anchored to TiO_2 nanocrystals, achieves very efficient sensitization over the whole visible range extending into the near-IR region down to 800 nm. The spectral response in the red and near-IR region is greatly enhanced compared to chemically stable standard semiconductors.[10,90,91] On the basis of its catalytic performance (up to 90% chemical yield for NIR excitation), this panchromatic photocatalyst is superior to all photocatalysts known thus far. It

enables oxidative cyanation reactions to the corresponding α-aminonitriles to proceed with high efficiency. α-Aminonitriles are useful intermediates for synthesis of a wide variety of compound classes. The reaction formally represents a photoassisted cross-dehydrogenative coupling (CDC)[92] of amines and HCN through sp^3 C–H bond activation adjacent to nitrogen followed by carbon-carbon bond formation under oxidative conditions. The discovery of enhanced light harvesting in the red and near-IR region through surface-binding of redox active ligands opens up the way to improve the overall yields in photocatalytic reactions. Thus, this class of functionalized semiconductors provides the conceptual basis for the design of new photocatalysts containing non-innocent donor ligands. This increases the molar extinction coefficient, permitting a reduction of nanoparticle catalyst concentration and an increase of the overall yields in photocatalytic reactions. Further improvements could be achieved by the use of microflow technology or through immobilized TiO_2 surfaces in continuous flow operations.[93]

EXPERIMENTAL SECTION

Materials. Unless otherwise stated, all chemicals and solvents were obtained from commercial suppliers and used without further purification. Oleic acid (technical grade, 90%) was obtained from Sigma-Aldrich. Titanium(IV) *n*-butoxide (99%) was purchased from Acros Organics. Oleylamine (>50.0% (GC)) was acquired from TCI. Deionized water (18.2 MΩ·cm) was obtained from a Milli-Q water purification system (Millipore Synergy 185).

Synthesis of Oleic Acid-Stabilized TiO_2 Nanoparticles (TiO_2-OA). TiO_2 nanoparticles were synthesized according to a previously reported procedure.[67] Titanium(IV) butoxide (2.89 g, 2.89 mL, 8.5 mmol, 1.0 eq.) was added to a mixture of oleic acid (14.41 g, 16.24 mL, 51 mmol, 6.0 eq.), oleylamine (9.09 g, 11.19 mL, 34 mmol, 4.0 eq.) and ethanol (7.83 g, 9.93 mL, 170 mmol, 20.0 eq., absolute grade). The mixture was stirred for 15 min and transferred into a 50 mL Teflon vessel. This vessel was placed into a 250 mL Teflon-lined stainless steel autoclave, already containing 34 mL of the hydrolysis solution of ethanol and water (96:4 v/v). The sealed autoclave was then heated at 180 °C for 18 h. After opening the cooled autoclave, the content of the inner vessel was decanted into a 50 mL centrifuge tube and the crude solid product was isolated by centrifugation (9000 rpm, 10 min) and dissolved in *n*-hexane (10 mL). The white solid residue at the bottom of the inner vessel was also dissolved in *n*-hexane (10–15 mL), transferred into a 50 mL centrifuge tube and precipitated by addition of ethanol (30–35 mL, technical grade). The white precipitate was isolated by centrifugation (9000 rpm, 10 min) and redissolved in *n*-hexane (5 mL).The combined NP solutions were further purified by repeated cycles of precipitation and dissolution (3 x 30/5 mL EtOH/*n*-hexane). The last dissolution step was usually carried out in $CHCl_3$ (3 mL) to

obtain a concentrated stock solution in a solvent that can be easily displaced for further reactions. The stock solution was stored in a tightly sealed amber glass vial with screw top, protected from sunlight, to extend its shelf life (stable solutions for at least up to a year). The exact concentration of the NP solution was determined from the remaining mass of an evaporated 100 µL aliquot (after several hours of drying at 80 °C). ^{1}H NMR (400 MHz, $CDCl_3$): δ = 5.7–5.0 (m, 2H, -CH=CH-), 2.4–0.6 (m, 31H, -CH_2- & -CH_3).

Synthesis of 6,7-Dimethoxy-2-methyl-1,2,3,4-tetrahydroisoquinoline (2). Homoveratrylamine (10.0 g, 55.2 mmol, 1.0 eq.), formic acid (16.5 g, 20.8 mL, 552 mmol, 10 eq.) and aqueous formaldehyde solution (37 wt.%, 20.5 mL, 5.0 eq.) were combined and heated for 6 h to 100 °C. The solution was made alkaline with sodium hydroxide solution (2 M) and extracted with ethyl acetate (3 x 50 mL). The combined organic layers were dried over sodium sulfate and concentrated in vacuo to yield the crude product. After purification by column chromatography (ethyl acetate/methanol = 2:1) the product was isolated as slightly yellow solid (10.96 g, 52.87 mmol, 96%). mp: 75.9–78.2 °C. Lit.: 78–90 °C.[66] R_f= 0.23 (ethyl acetate/methanol = 2:1). IR (ATR): ν = 2936 (s), 2834 (m), 2768 (m), 1518 (vs), 1463 (s), 1374 (s), 1258 (vs), 1228 (vs), 1138 (vs), 1104 (s), 1013 (m) cm^{-1}. ^{1}H NMR, COSY (300 MHz, $CDCl_3$): δ = 6.59 (s, 1H, H-5), 6.51 (s, 1H, H-8), 3.84 (s, 3H, OCH_3), 3.83 (s, 3H, OCH_3). 3.50 (s, 2H, H-1), 2.84 (t, $^{3}J_{H\text{-}4,\ H\text{-}3}$ = 5.9 Hz, 2H, H-4), 2.66 (t, $^{3}J_{H\text{-}3,\ H\text{-}4}$ = 5.9 Hz, 2H, H-3), 2.45 (s, 3H, NCH_3). ^{13}C NMR, HMBC, HSQC (75 MHz, $CDCl_3$): δ = 147.6, 147.3 (C-6, C-7), 126.7 (C-8a), 125.8 (C-4a), 111.5 (C-5), 109.4 (C-8), 57.7 (C-1), 56.1, 56.0 (2 x OCH_3), 53.1 (C-3), 46.2 (NCH_3), 29.0 (C-4). ESI-MS: m/z = 207.0 ([M+H$^+$], 100%). The spectral data match those reported in the literature.[66,94]

Synthesis of 6,7-Dimethoxy-2-methylisoquinolinium Chloride (3). 6,7-Dimethoxy-2-methyl-1,2,3,4-tetrahydroisoquinoline (1.00 g, 4.83 mmol, 1.0 eq) was dissolved in acetonitrile (80 mL) and DDQ was added (2.19 g, 9.65 mmol, 2.0 eq.). The reaction mixture was refluxed and every 24 h additional DDQ (2.0 eq) was added. After 4 days and 8.0 eq. of DDQ added, LCMS indicated full conversion. The solvent was evaporated in vacuo and the solid residue was dissolved in diluted hydrochloric acid (2 M, 50 mL). The aqueous solution was extracted with diethyl ether in a Kutscher-Steudel apparatus for two days (note: ethyl acetate, chloroform or dichlormethan are not suitable in this case). The organic extract was dried over sodium sulfate and concentrated in vacuo to yield the pure iminium salt (1.04 g, 4.35 mmol, 90%). mp: 301–311 °C (decomposition). Lit. (iodide salt): 235–238 °C.[95] ^{1}H NMR, COSY (300 MHz, D_2O): δ = 9.14 (s, 1H,), 8.21 (dd, $^{3}J_{H\text{-}3,\ H\text{-}4}$ = 6.8 Hz, $^{4}J_{H\text{-}3,\ H\text{-}1}$ = 1.4 Hz, 1H, H-3), 8.03 (d, $^{3}J_{H\text{-}4,\ H\text{-}3}$ = 6.8 Hz, 1H, H-4), 7.48 (s, 1H, H-8), 7.40 (s, 1H, H-5), 4.37 (s, 3H, NCH_3), 4.00 (s, 3H, C6-OCH_3), 3.97 (s, 3H, C7-OCH_3). ^{13}C NMR, HMBC, HSQC (75 MHz, D_2O): δ = 157.0 (C-6), 152.1 (C-7), 145.1 (C-1), 135.3 (C-4a), 133.7 (C-3), 124.0 (C-8a), 123.5 (C-4), 106.6 (C-8), 105.4 (C-5), 56.6 (C6-OCH_3), 56.2 (C7-OCH_3), 47.1

(NCH_3). ESI-MS: m/z = 204.1 ([M^+], 100%). The spectral data match those reported in the literature.[96]

Synthesis of 6,7-Dihydroxy-2-methylisoquinolinium Chloride (DHMIQ). 6,7-Dimethoxy-2-methylisoquinolinium chloride (890 mg, 3.71 mmol, 1.0 eq.) was dissolved in conc. hydrochloric acid (20 mL) and heated in a monomode microwave reactor (8 h, 140 °C, 20 bar, 45 W; ramp: 20 min). The solution was concentrated into dryness in vacuo to yield DHMIQ (786 mg, 3.71 mmol, quant.). mp: 265–271 °C (decomposition). IR (ATR): ν = 2970 (w_B), 1624 (w), 1529 (w), 1483 (m), 1436 (m), 1391 (w), 1371 (w), 1298 (s), 1173 (s), 1156 (s), 871 (s), 628 (m), 576 (m), 471 (vs) cm^{-1}. ^1H NMR, COSY (300 MHz, D_2O): δ = 8.96 (s, 1H, H-1), 8.04 (dd, $^3J_{H\text{-}3,\,H\text{-}4}$ = 6.8 Hz, $^4J_{H\text{-}3,\,H\text{-}1}$ = 1.3 Hz, 1H, H-3), 7.84 (d, $^3J_{H\text{-}4,\,H\text{-}3}$ = 6.8 Hz, 1H, H-4), 7.30 (s, 1H, H-8), 7.18 (s, 1H, H-5), 4.30 (s, 3H, NCH_3). ^{13}C NMR, HMBC, HSQC (75 MHz, D_2O): δ = 155.2 (C-6), 149.3 (C-7), 144.7 (C-1), 134.5 (C-4a), 132.6 (C-3), 123.6 (C-8a), 122.9 (C-4), 110.5 (C-8), 108.7 (C-5), 46.9 (NCH_3). ESI-HRMS: calcd for $[C_{10}H_{10}NO_2]^+$: m/z = 176.0706, found: 176.0711.

Synthesis of TiO_2-DHMIQ Nanoparticles. First, an aliquot of the titania stock solution, corresponding to a NP amount of 100 mg, was transferred into a 2 mL microcentrifuge tube, precipitated with excess acetone, centrifuged (14800 rpm, 3 min) and redissolved in THF (1.0 mL). The DHMIQ ligand (50 mg, 0.24 mmol) was dissolved in a ternary solvent mixture of water (1.0 mL), MeOH (0.5 mL) and THF (1.5 mL). The NP solution was added to the ligand solution, forming an opaque suspension, which was then sonicated (280 W) at 40 °C for 1 h. The reaction mixture was centrifuged (9000 rpm, 15 min), the yellow supernatant was discarded and the brownish-red pellet was dried in rough vacuum (30 mbar, 10 min). The dried NPs were redissolved in a minimum amount of water (0.2 mL) with the aid of vortexing and sonication. After precipitation with excess THF (3.0 mL), the NPs were separated by centrifugation (9000 rpm, 10 min) and dried in low vacuum. The DHMIQ-functionalized TiO_2 NPs were further purified by repeated cycles of dissolution, precipitation and drying as described above (6 iterations in total). To obtain an ^1H NMR spectrum of the DHMIQ-functionalized TiO_2 NPs that is not obscured by large residual signals of the undeuterated solvents, the penultimate dissolution step was performed in D_2O, followed by the ultimate precipitation step with acetone-d_6 and redissolution of the dried NPs in D_2O. ^1H NMR (400 MHz, D_2O): δ = 9.4–5.2 (m, 5H, Ar-H), 5.2–2.5 (m, 3H, NCH_3).

Synthesis of Ligand-Stripped TiO_2 Nanoparticles (TiO_2-TMA). First, an aliquot of the titania stock solution, corresponding to a NP amount of 200 mg, was precipitated with excess acetone, centrifuged (14800 rpm, 3 min) and redissolved in THF (1.0 mL). Tetramethylammonium hydroxide pentahydrate ($TMAH{\cdot}5H_2O$, 1.0 g, 5.5 mmol) was dissolved in 1.0 mL H_2O and added to the NP solution. The combined solution was shaken and sonicated (280 W) at 40 °C for 1 h to afford a biphasic clear mixture. Addition of MeOH (2.0 mL) caused the phases to merge and the NPs were then precipitated with excess THF (15 mL). The mixture was centrifuged (9000 rpm, 10 min),

the yellow supernatant was discarded and the whitish pellet was dried in rough vacuum (30 mbar, 10 min). The dried NPs were redissolved in a minimum amount of water (0.2 mL) with the aid of vortexing and sonication. After precipitation with excess THF (3.0 mL), the NPs were again separated by centrifugation (9000 rpm, 10 min) and dried in rough vacuum. The ligand-stripped TiO_2-TMA NPs were further purified by repeated cycles of dissolution, precipitation and drying as described above (4 iterations in total). To obtain an ^1H NMR spectrum of the TiO_2-TMA NPs that is not obscured by large residual signals of the undeuterated solvents, the penultimate dissolution step was performed in D_2O, followed by the ultimate precipitation step with acetone-d_6 and redissolution of the dried NPs in D_2O. ^1H NMR (400 MHz, D_2O): δ = 3.6–2.8 (s, 12H, $N(CH_3)_4$).

General Procedure for the Photocyanation of Amines. An aliquot of the TiO_2-DHMIQ solution (2.5 mg catalyst) was transferred in a reaction vial and freeze dried. The dried catalyst was suspended with acetonitrile (4.0 mL) and the substrate (0.239 mmol, 1.0 eq.) was added. Oxygen was bubbled through the solution for one minute to saturate the solution. Trimethylsilyl cyanide (3.0 eq.) was added and the vial was closed tight. The solution was irradiated, if not stated otherwise, for 3 h, poured in concentrated $NaHCO_3$ solution (30 mL) and extracted with CH_2Cl_2 (3 x 20 mL). The combined organic layers were dried over Na_2SO_4 and the solvent was evaporated under reduced pressure to obtain the crude product. The pure product was isolated by filtration through a plug of aluminum oxide (basic) using CH_2Cl_2 as the eluent or by column chromatography.

Further details of the experimental setup and substrate-specific procedures are provided in the Supporting Information.

ASSOCIATED CONTENT

(1) Synthesis of TiO_2-DHMIQ, (2) nanoparticle characterization, (3) general procedure and setup, (4) analytical data, (5) reaction screening, (6) additional NMR spectra.

AUTHOR INFORMATION

Corresponding Authors: opatz@uni-mainz.de and tremel@uni-mainz.de. The authors declare no competing financial interest.

ACKNOWLEDGEMENTS

E. Schechtel is recipient of a Max Planck Graduate Center (MPGC) fellowship and a collegiate of the MAINZ Graduate School of the State of Rhineland-Palatinate. This work was supported by the Rhineland-Palatinate Natural Products Research Center. We thank R. Jung-Pothmann for X-ray

diffraction measurements. The microscopy equipment is operated by the electron microscopy center, Mainz, (EMZM) supported by the Johannes Gutenberg-University.

REFERENCES

(1) Kisch, H. *Angew. Chem., Int. Ed.* **2013**, *52*, 812–847.
(2) Kisch, H. *Acc. Chem. Res.* **2017**, *50*, 1002–1010.
(3) Rusina, O.; Linnik, O.; Eremenko, A.; Kisch, H. *Chem. - Eur. J.* **2003**, *9*, 561–565.
(4) Balzani, V.; Bergamini, G.; Ceroni, P. *Angew. Chem., Int. Ed.* **2015**, *54*, 11320–11337.
(5) Soffer, B. H.; Lynch, D. K. *Am. J. Phys.* **1999**, *67*, 946–953.
(6) Taiz, L.; Zeiger, E.; Møller, I. M.; Murphy, A. *Plant Physiology and Development*, 6th ed.; Oxford University Press, Inc.: Oxford, 2018.
(7) Prier, C. K.; Rankic, D. A.; MacMillan, D. W. C. *Chem. Rev.* **2013**, *113*, 5322–5363.
(8) Senaweera, S.; Weaver, J. D. *J. Am. Chem. Soc.* **2016**, *138*, 2520–2523.
(9) Sang, L.; Zhao, Y.; Burda, C. *Chem. Rev.* **2014**, *114*, 9283–9318.
(10) Schneider, J.; Matsuoka, M.; Takeuchi, M.; Zhang, J.; Horiuchi, Y.; Anpo, M.; Bahnemann, D. W. *Chem. Rev.* **2014**, *114*, 9919–9986.
(11) Su, R.; Dimitratos, N.; Liu, J.; Carter, E.; Althahban, S.; Wang, X.; Shen, Y.; Wendt, S.; Wen, X.; Niemantsverdriet, J. W.; Iversen, B. B.; Kiely, C. J.; Hutchings, G. J.; Besenbacher, F. *ACS Catal.* **2016**, *6*, 4239–4247.
(12) Caronna, T.; Gambarotti, C.; Palmisano, L.; Punta, C.; Recupero, F. *Chem. Commun.* **2003**, 2350–2351.
(13) Fagnoni, M.; Dondi, D.; Ravelli, D.; Albini, A. *Chem. Rev.* **2007**, *107*, 2725–2756.
(14) Ravelli, D.; Dondi, D.; Fagnoni, M.; Albini, A. *Chem. Soc. Rev.* **2009**, *38*, 1999–2011.
(15) Yoon, T. P.; Ischay, M. A.; Du, J. *Nat. Chem.* **2010**, *2*, 527–532.
(16) Jin, J.; MacMillan, D. W. C. *Nature* **2015**, *525*, 87–90.
(17) Jin, H.; Huang, L.; Xie, J.; Rudolph, M.; Rominger, F.; Hashmi, A. S. K. *Angew. Chem., Int. Ed.* **2016**, *55*, 794–797.
(18) Ushakov, D. B.; Gilmore, K.; Kopetzki, D.; McQuade, D. T.; Seeberger, P. H. *Angew. Chem., Int. Ed.* **2014**, *53*, 557–561.
(19) Orejarena Pacheco, J. C.; Lipp, A.; Nauth, A. M.; Acke, F.; Dietz, J.-P.; Opatz, T. *Chem. - Eur. J.* **2016**, *22*, 5409–5415.
(20) Hernández-Alonso, M. D.; Fresno, F.; Suárez, S.; Coronado, J. M. *Energy Environ. Sci.* **2009**, *2*, 1231–1257.
(21) Yoon, H.-S.; Ho, X.-H.; Jang, J.; Lee, H.-J.; Kim, S.-J.; Jang, H.-Y. *Org. Lett.* **2012**, *14*, 3272–3275.
(22) Nazeeruddin, M. K.; Péchy, P.; Renouard, T.; Zakeeruddin, S. M.; Humphry-Baker, R.; Comte, P.; Liska, P.; Cevey, L.; Costa, E.; Shklover, V.; Spiccia, L.; Deacon, G. B.; Bignozzi, C. A.; Grätzel, M. *J. Am. Chem. Soc.* **2001**, *123*, 1613–1624.
(23) Tian, H.; Yang, X.; Chen, R.; Hagfeldt, A.; Sun, L. *Energy Environ. Sci.* **2009**, *2*, 674–677.
(24) Cid, J.-J.; Yum, J.-H.; Jang, S.-R.; Nazeeruddin, M. K.; Martínez-Ferrero, E.; Palomares, E.; Ko, J.; Grätzel, M.; Torres, T. *Angew. Chem., Int. Ed.* **2007**, *46*, 8358–8362.
(25) Zhang, G.; Kim, G.; Choi, W. *Energy Environ. Sci.* **2014**, *7*, 954–966.
(26) Ooyama, Y.; Kanda, M.; Uenaka, K.; Ohshita, J. *ChemPhysChem* **2015**, *16*, 3049–3057.

(27) Ooyama, Y.; Yamaji, K.; Ohshita, J. *Mater. Chem. Front.* **2017**, *1*, 2243–2255.
(28) Wada, K.; Yoshida, K.; Takatani, T.; Watanabe, Y. *Appl. Catal., A* **1993**, *99*, 21–36.
(29) Zeug, N.; Bücheler, J.; Kisch, H. *J. Am. Chem. Soc.* **1985**, *107*, 1459–1465.
(30) Zhang, Y.; Zhang, N.; Tang, Z.-R.; Xu, Y.-J. *Chem. Sci.* **2012**, *3*, 2812–2822.
(31) Pal, A.; Ghosh, I.; Sapra, S.; König, B. *Chem. Mater.* **2017**, *29*, 5225–5231.
(32) Su, F.; Mathew, S. C.; Möhlmann, L.; Antonietti, M.; Wang, X.; Blechert, S. *Angew. Chem., Int. Ed.* **2011**, *50*, 657–660.
(33) Yuan, R.; Fan, S.; Zhou, H.; Ding, Z.; Lin, S.; Li, Z.; Zhang, Z.; Xu, C.; Wu, L.; Wang, X.; Fu, X. *Angew. Chem., Int. Ed.* **2013**, *52*, 1035–1039.
(34) Füldner, S.; Pohla, P.; Bartling, H.; Dankesreiter, S.; Stadler, R.; Gruber, M.; Pfitzner, A.; König, B. *Green Chem.* **2011**, *13*, 640–643.
(35) Füldner, S.; Mild, R.; Siegmund, H. I.; Schroeder, J. A.; Gruber, M.; König, B. *Green Chem.* **2010**, *12*, 400–406.
(36) Zhang, M.; Chen, C.; Ma, W.; Zhao, J. *Angew. Chem., Int. Ed.* **2008**, *47*, 9730–9733.
(37) Füldner, S.; Mitkina, T.; Trottmann, T.; Frimberger, A.; Gruber, M.; König, B. *Photochem. Photobiol. Sci.* **2011**, *10*, 623–625.
(38) Peter, L. *Acc. Chem. Res.* **2009**, *42*, 1839–1847.
(39) Grätzel, M. *Acc. Chem. Res.* **2009**, *42*, 1788–1798.
(40) Nour-Mohhamadi, F.; Nguyen, S. D.; Boschloo, G.; Hagfeldt, A.; Lund, T. *J. Phys. Chem. B* **2005**, *109*, 22413–22419.
(41) Li, C.; Yum, J.-H.; Moon, S.-J.; Herrmann, A.; Eickemeyer, F.; Pschirer, N. G.; Erk, P.; Schöneboom, J.; Müllen, K.; Grätzel, M.; Nazeeruddin, M. K. *ChemSusChem* **2008**, *1*, 615–618.
(42) Ye, S.; Kathiravan, A.; Hayashi, H.; Tong, Y.; Infahsaeng, Y.; Chabera, P.; Pascher, T.; Yartsev, A. P.; Isoda, S.; Imahori, H.; Sundström, V. *J. Phys. Chem. C* **2013**, *117*, 6066–6080.
(43) Materna, K. L.; Crabtree, R. H.; Brudvig, G. W. *Chem. Soc. Rev.* **2017**, *46*, 6099–6110.
(44) Ma, W.; Han, D.; Zhou, M.; Sun, H.; Wang, L.; Dong, X.; Niu, L. *Chem. Sci.* **2014**, *5*, 3946–3951.
(45) Caputo, C. A.; Wang, L.; Beranek, R.; Reisner, E. *Chem. Sci.* **2015**, *6*, 5690–5694.
(46) Baciocchi, E.; Giacco, T. Del; Elisei, F.; Gerini, M. F.; Guerra, M.; Lapi, A.; Liberali, P. *J. Am. Chem. Soc.* **2003**, *125*, 16444–16454.
(47) Baciocchi, E.; Del Giacco, T.; Lanzalunga, O.; Mencarelli, P.; Procacci, B. *J. Org. Chem.* **2008**, *73*, 5675–5682.
(48) Santamaria, J.; Kaddachi, M. T.; Rigaudy, J. *Tetrahedron Lett.* **1990**, *31*, 4735–4738.
(49) Jørgensen, C. K. *Coord. Chem. Rev.* **1966**, *1*, 164–178.
(50) Pierpont, C. G.; Lange, C. W. *Prog. Inorg. Chem.* **1994**, *41*, 331–442.
(51) Chirik, P. J.; Wieghardt, K. *Science* **2010**, *327*, 794–795.
(52) Lyaskovskyy, V.; de Bruin, B. *ACS Catal.* **2012**, *2*, 270–279.
(53) Zorn, M.; Weber, S. A. L.; Tahir, M. N.; Tremel, W.; Butt, H.-J.; Berger, R.; Zentel, R. *Nano Lett.* **2010**, *10*, 2812–2816.
(54) Kaim, W. *Inorg. Chem.* **2011**, *50*, 9752–9765.
(55) Praneeth, V. K. K.; Ringenberg, M. R.; Ward, T. R. *Angew. Chem., Int. Ed.* **2012**, *51*, 10228–10234.
(56) Sang, Y.; Liu, H.; Umar, A. *ChemCatChem* **2015**, *7*, 559–573.
(57) Tahir, M. N.; Natalio, F.; Cambaz, M. A.; Panthöfer, M.; Branscheid, R.; Kolb, U.; Tremel, W. *Nanoscale* **2013**, *5*, 9944–9949.

(58) Piera, J.; Bäckvall, J.-E. *Angew. Chem., Int. Ed.* **2008**, *47*, 3506–3523.
(59) Zeitler, K. *Angew. Chem., Int. Ed.* **2009**, *48*, 9785–9789.
(60) Wang, Y.; Hang, K.; Anderson, N. A.; Lian, T. *J. Phys. Chem. B* **2003**, *107*, 9434–9440.
(61) Duthaler, R. O. *Tetrahedron* **1994**, *50*, 1539–1650.
(62) North, M. *Angew. Chem., Int. Ed.* **2004**, *43*, 4126–4128.
(63) Liu, L.; Wang, Z.; Fu, X.; Yan, C.-H. *Org. Lett.* **2012**, *14*, 5692–5695.
(64) Otto, N.; Opatz, T. *Chem. - Eur. J.* **2014**, *20*, 13064–13077.
(65) Murahashi, S.-I.; Zhang, D. *Chem. Soc. Rev.* **2008**, *37*, 1490–1501.
(66) Ruchirawat, S.; Chaisupakitsin, M.; Patranuwatana, N.; Cashaw, J. L.; Davis, V. E. *Synth. Commun.* **1984**, *14*, 1221–1228.
(67) Dinh, C.-T.; Nguyen, T.-D.; Kleitz, F.; Do, T.-O. *ACS Nano* **2009**, *3*, 3737–3743.
(68) Hens, Z.; Martins, J. C. *Chem. Mater.* **2013**, *25*, 1211–1221.
(69) Tong, L.; Lu, E.; Pichaandi, J.; Cao, P.; Nitz, M.; Winnik, M. A. *Chem. Mater.* **2015**, *27*, 4899–4910.
(70) Zeininger, L.; Portilla, L.; Halik, M.; Hirsch, A. *Chem. - Eur. J.* **2016**, *22*, 13506–13512.
(71) Linsebigler, A. L.; Lu, G.; Yates, J. T. *Chem. Rev.* **1995**, *95*, 735–758.
(72) Euliss, L. E.; Grancharov, S. G.; O'Brien, S.; Deming, T. J.; Stucky, G. D.; Murray, C. B.; Held, G. A. *Nano Lett.* **2003**, *3*, 1489–1493.
(73) Salgueiriño-Maceira, V.; Liz-Marzán, L. M.; Farle, M. *Langmuir* **2004**, *20*, 6946–6950.
(74) Creutz, C.; Chou, M. H. *Inorg. Chem.* **2008**, *47*, 3509–3514.
(75) Mi, J.-L.; Jensen, K. M. Ø.; Tyrsted, C.; Bremholm, M.; Iversen, B. B. *CrystEngComm* **2015**, *17*, 6868–6877.
(76) Lang, X.; Zhao, J.; Chen, X. *Angew. Chem., Int. Ed.* **2016**, *55*, 4697–4700.
(77) Smith, J. G.; Jain, P. K. *J. Am. Chem. Soc.* **2016**, *138*, 6765–6773.
(78) Borgias, B. A.; Cooper, S. R.; Koh, Y. B.; Raymond, K. N. *Inorg. Chem.* **1984**, *23*, 1009–1016.
(79) Wang, J.; Tahir, M. N.; Kappl, M.; Tremel, W.; Metz, N.; Barz, M.; Theato, P.; Butt, H.-J. *Adv. Mater.* **2008**, *20*, 3872–3876.
(80) Dondi, D.; Buttafava, A.; Zeffiro, A.; Bracco, S.; Sozzani, P.; Faucitano, A. *J. Phys. Chem. A* **2013**, *117*, 3304–3318.
(81) Estévez, C. M.; Dmitrenko, O.; Winter, J. E.; Bach, R. D. *J. Org. Chem.* **2000**, *65*, 8629–8639.
(82) Hu, J.; Wang, J.; Nguyen, T. H.; Zheng, N. *Beilstein J. Org. Chem.* **2013**, *9*, 1977–2001.
(83) Nelsen, S. F.; Ippoliti, J. T. *J. Am. Chem. Soc.* **1986**, *108*, 4879–4881.
(84) Dombrowski, G. W.; Dinnocenzo, J. P.; Zielinski, P. A.; Farid, S.; Wosinska, Z. M.; Gould, I. R. *J. Org. Chem.* **2005**, *70*, 3791–3800.
(85) Nazran, A. S.; Griller, D. *J. Am. Chem. Soc.* **1983**, *105*, 1970–1971.
(86) Lal, J.; Green, R. *J. Polym. Sci.* **1955**, *17*, 403–409.
(87) Kohls, P.; Jadhav, D.; Pandey, G.; Reiser, O. *Org. Lett.* **2012**, *14*, 672–675.
(88) Cai, S.; Zhao, X.; Wang, X.; Liu, Q.; Li, Z.; Wang, D. Z. *Angew. Chem., Int. Ed.* **2012**, *51*, 8050–8053.
(89) Wang, Z.; Lang, X. *Appl. Catal. B Environ.* **2018**, *224*, 404–409.
(90) Duncan, W. R.; Prezhdo, O. V. *Annu. Rev. Phys. Chem.* **2007**, *58*, 143–184.
(91) Molet, P.; Garcia-Pomar, J. L.; Matricardi, C.; Garriga, M.; Alonso, M. I.; Mihi, A. *Adv. Mater.* **2018**, *30*, 1705876.
(92) Girard, S. A.; Knauber, T.; Li, C.-J. *Angew. Chem., Int. Ed.* **2014**, *53*, 74–100.
(93) Su, Y.; Straathof, N. J. W.; Hessel, V.; Noël, T. *Chem. - Eur. J.* **2014**, *20*, 10562–10589.

(94) Katritzky, A. R.; He, H.-Y.; Jiang, R.; Long, Q. *Tetrahedron: Asymmetry* **2001**, *12*, 2427–2434.
(95) Knabe, J.; Roloff, H. *Chem. Ber.* **1964**, *97*, 3452–3455.
(96) Janssen, R. H. A. M.; Ch. Lousberg, R. J. J.; Wijkens, P.; Kruk, C.; Theuns, H. G. *Phytochemistry* **1989**, *28*, 2833–2839.

Received: ((will be filled in by the editorial staff))
Revised: ((will be filled in by the editorial staff))
Published online: ((will be filled in by the editorial staff))

Graphical Abstract

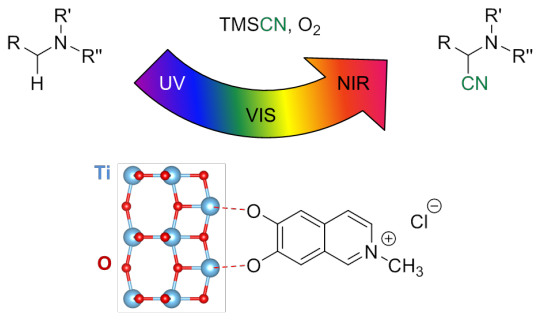

nano anatase TiO_2 + photosensitive surface ligand